

Iron–Sulfur Clusters of Biotin Synthase In Vivo: A Mössbauer Study[†]

Rüdiger Benda,[‡] Bernadette Tse Sum Bui,[§] Volker Schünemann,[‡] Dominique Florentin,[§] Andrée Marquet,^{*,§} and Alfred X. Trautwein^{*,‡}

Institut für Physik, Universität zu Lübeck, Ratzeburger Allee 160, 23538 Lübeck, Germany, and Laboratoire de Chimie Organique Biologique, Université Paris VI, UMR CNRS 7613, 4 Place Jussieu, 75252 Paris Cedex 05, France

Received August 6, 2002; Revised Manuscript Received October 8, 2002

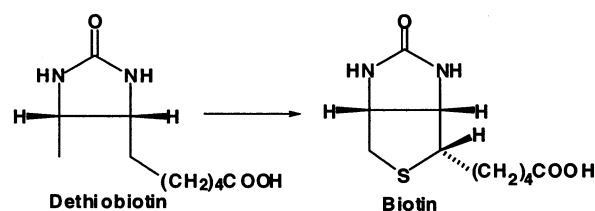
ABSTRACT: Biotin synthase, the enzyme that catalyzes the last step of the biosynthesis of biotin, contains only $[2\text{Fe-2S}]^{2+}$ clusters when isolated under aerobic conditions. Previous results showed that reconstitution with an excess of FeCl_3 and Na_2S under reducing and anaerobic conditions leads to either $[4\text{Fe-4S}]^{2+}$, $[4\text{Fe-4S}]^+$, or a mixture of $[4\text{Fe-4S}]^{2+}$ and $[2\text{Fe-2S}]^{2+}$ clusters. To determine whether any of these possibilities or other different cluster configuration could correspond to the physiological in vivo state, we have used ^{57}Fe Mössbauer spectroscopy to investigate the clusters of biotin synthase in whole cells. The results show that, in aerobically grown cells, biotin synthase contains a mixture of $[4\text{Fe-4S}]^{2+}$ and $[2\text{Fe-2S}]^{2+}$ clusters. A mixed $[4\text{Fe-4S}]^{2+}:[2\text{Fe-2S}]^{2+}$ cluster form has already been observed under certain in vitro conditions, and it has been proposed that both clusters might each play a significant role in the mechanism of biotin synthase. Their presence in vivo is now another argument in favor of this mixed cluster form.

Biotin synthase (BS)¹ catalyses the final step of the biotin biosynthetic pathway, i.e., the insertion of a sulfur atom into dethiobiotin, as shown in Scheme 1. Aerobically purified recombinant BS from *Escherichia coli* is a homodimeric protein that contains a $[2\text{Fe-2S}]^{2+}$ cluster (1–3). However, the iron and sulfide contents of the purified enzyme can vary from a maximum of $1.5[2\text{Fe-2S}]^{2+}$ to a minimum of $0.25[2\text{Fe-2S}]^{2+}$ per monomer as judged by the different reports (4–6). The reason for this discrepancy is still unknown, but one possible explanation might be that the apo-polypeptide is not properly folded to accommodate the $[\text{Fe-S}]$ clusters.

In vitro activity requires the absolute presence of *S*-adenosylmethionine (AdoMet) (7, 8) and a reducing system [*NADPH*, flavodoxin (9), flavodoxin reductase (10)] whose role is to transfer an electron to the $[\text{Fe-S}]$ center, which is then able to reductively cleave AdoMet, generating methionine and a 5'-deoxyadenosyl radical (DOA[•]) (11).

By using deuterated dethiobiotin samples, we have demonstrated that the DOA[•] abstracts a hydrogen atom directly from the substrate and that one DOA[•] is involved in the formation of each C–S bond (12). We have also shown that

Scheme 1: Reaction Catalyzed by Biotin Synthase



BS in which the $[2\text{Fe-2S}]^{2+}$ cluster was labeled with ^{34}S by reconstitution donates ^{34}S to biotin in an in vitro assay (13). Hence, we proposed that the source of sulfur was very likely the $[\text{Fe-S}]$ center. These two crucial findings in the mechanism of BS are depicted in Scheme 2.

The conditions of the enzymatic assay being reducing, a wide variety of spectroscopic methods has been employed to characterize the reduced state of the $[\text{Fe-S}]$ centers in BS. The first detailed investigation was carried out using a combination of UV–visible, EPR, resonance Raman, and variable temperature magnetic circular dichroism spectroscopies by the group of Johnson (2), who showed that anaerobic reduction with dithionite results in the conversion of two $[2\text{Fe-2S}]^{2+}$ clusters to one $[4\text{Fe-4S}]^{2+}$ or $[4\text{Fe-4S}]^+$ per dimer depending on whether the medium contains ethylene glycol or not. However, no significant difference in enzymatic activities was observed in assays starting from the three different cluster states, which probably means that the transformation occurs during the reaction.

Later, by using Mössbauer spectroscopy, which allows quantification of the different iron species, we confirmed this $[2\text{Fe-2S}]^{2+}$ to $[4\text{Fe-4S}]^{2+}$ transformation during dithionite reduction in a glycerol (55%, v/v) medium but in addition noticed that there was partial destruction to Fe^{2+} , indicating that the conversion was not quantitative. This cluster transformation was reversible, and during exposure to air, the $[4\text{Fe-4S}]^{2+}$ was quantitatively reconverted to $[2\text{Fe-2S}]^{2+}$ clusters (3).

[†] This research has been supported by the French-German Cooperation Program, Procope (00373PJ) and by the Ministère de l'Éducation Nationale de la Recherche et de la Technologie (98C0326).

* To whom correspondence should be addressed. (A.M.) telephone: +33 1 44 27 55 64; fax: +33 1 44 27 71 50; e-mail: marquet@ccr.jussieu.fr. (A.X.T.) telephone: +49 451 500 4200; fax: +49 451 500 4214; e-mail: trautwein@physik.uni-luebeck.de.

[‡] Universität zu Lübeck.

[§] Université Paris VI.

¹ Abbreviations: AdoMet, *S*-adenosylmethionine; BS, biotin synthase; BS⁺, cells or crude extracts containing overexpressed BS; WT, cells of the wild-type strain; DEAE, diethylaminoethyl; DOA[•], 5'-deoxyadenosyl radical; DOAH, 5'-deoxyadenosine; DTT, dithiothreitol; EPR, electron paramagnetic resonance; $[\text{Fe-S}]$, iron–sulfur cluster; FNR, fumarate nitrate reduction; IPTG, isopropyl- β -D-thiogalactoside; *NADPH*, nicotinamide adenine dinucleotide phosphate, reduced form; TB, terrific broth; Tris-HCl, tris(hydroxymethyl)aminomethane hydrochloride.

The diagram illustrates the biotin biosynthetic pathway in bacteria. It begins with the reduction of NADPH to NADP⁺ by Flavodoxin reductase, which then reduces Flavodoxin ox to Flavodoxin H₂. Flavodoxin H₂ reduces [Fe-S]_{ox} to [Fe-S]_{red}. [Fe-S]_{red} is then used by Biotin synthase to convert Methionine to DOA (DOA-CH₂-CH₂-CH₂-COO⁻). DOA is then converted to Dethiobiotin (DOA-CH₂-CH₂-CH₂-COO⁻). Dethiobiotin is converted to DOAH (DOAH-CH₂-CH₂-CH₂-COO⁻). DOAH is then converted to Biotin (Biotin-CH₂-CH₂-CH₂-COO⁻). The diagram shows the chemical structures of Methionine, DOA, Dethiobiotin, DOAH, and Biotin, along with the intermediates [Fe-S]_{ox} and [Fe-S]_{red}.

From all the above findings taken together, the only conclusion that can be drawn without ambiguity is the omnipresence of the $[4\text{Fe-4S}]^{2+}$ under reducing and anaerobic conditions and its sensitivity to oxygen. Besides this, which cluster composition, among the above possibilities, reflects the precise state in *in vitro* biotin synthase and *a priori in vivo* cannot be inferred. Hence, in an attempt to answer this question, we have undertaken Mössbauer studies of whole cells containing overexpressed biotin synthase (BS+). As reference, whole cells of the wild-type strain (WT) grown

Preparation of Whole Cells. *E. coli* TK101 strains, one bearing the plasmid pI₃BLS₂ overexpressing biotin synthase (BS+) (17) and the other one from which the plasmid has been removed (WT) were generous gifts from Pr. Y. Izumi (Tottori University, Japan). ⁵⁷Fe was incorporated into BS by growing the *E. coli* strains on medium enriched with ⁵⁷FeCl₃. The medium that we normally employ in the laboratory for the cultivation of TK101pI₃BLS₂ is TB (12 g of tryptone (Organotechnie), 24 g of yeast extract (Organotechnie), 4 mL of glycerol, 2.31 g of KH₂PO₄, and 12.54 g of K₂HPO₄ in 1 L, pH 7.0). This medium contains approximately 27 μM ⁵⁶Fe from the yeast extract in addition to 3 μM from tryptone. Generally, for in vivo ⁵⁷Fe labeling, cells are grown in M9 minimal media (18). But due to the

poor growth of our strain in this medium, we employed our usual TB medium and supplemented it with $\sim 30 \mu\text{M}$ $^{57}\text{FeCl}_3$.

A preculture of *E. coli* TK101pI₃BLS₂ was grown aerobically overnight at 37 °C in 5 mL of TB medium containing 31 μM $^{57}\text{FeCl}_3$ in the presence of 100 $\mu\text{g/mL}$ of ampicillin. This preculture was then used to inoculate 800 mL of medium in 2-L flasks, and the culture was left to agitate vigorously at 37 °C. At $A_{600} \sim 1$, 100 μM isopropyl- β -D-thiogalactoside (IPTG) was added, and cultivation was continued overnight to reach the stationary phase. The BS WT strain was grown under the same conditions except that no ampicillin and no IPTG were added. The cells were harvested by centrifugation and washed with buffer A (50 mM Tris-HCl, pH 7.5) containing 0.1 M KCl followed by buffer A containing 2 mM DTT. One gram of wet-packed cells of BS+ and WT were then transferred separately to 1-mL Mössbauer sample holders and frozen in liquid nitrogen until measurement.

Preparation of Cell-Free Extracts and Pure Biotin Synthase. To minimize the presence of oxygen, all buffers used during enzyme preparations were saturated with argon. BS+ cells were suspended in buffer A containing 2 mM DTT and 0.2 mM phenylmethane sulfonyl fluoride and disrupted with an ultrasonic oscillator (Vibracell VC 600, Fisher Bioblock Scientific). Cell debris were removed by centrifugation at 30000g for 20 min. The supernatant solution constitutes the cell-free extracts. As this fraction was too dilute for Mössbauer measurements, it was further concentrated on an ultrafiltration device with a molecular weight cutoff of 30 kDa (Centriprep YM-30, Millipore). This fraction was termed crude BS+.

BS was purified from the cell-free extracts, with some modifications, as already described (1). An anion-exchange (DEAE), a hydrophobic (phenyl), and another anion-exchange (Q) chromatographic columns were successively employed. The as-purified protein sample was in 50 mM Tris-HCl + 2 mM DTT (pH 7.5). A 800- μL sample of 48 mg of protein/mL of crude BS+ and 210 μL of 50 mg/mL of pure BS were then transferred to Mössbauer cups and frozen in liquid nitrogen until measurement.

Analytical Methods. Protein concentration was measured by the method of Bradford (19) using bovine serum albumin as a standard. Iron was assayed by the method of Fish (20), and inorganic sulfide was quantified as described by Beinert (21).

Mössbauer Spectroscopy. Mössbauer spectra were recorded using a spectrometer in the constant acceleration mode. Isomer shifts are given relative to α -Fe at room temperature. The spectra obtained at 20 mT were measured in a He-bath cryostat (Oxford MD 306) equipped with a pair of permanent magnets. High-field measurements (7 T) were performed with a cryostat equipped with a superconducting magnet (Oxford Instruments, Spectromag 4000). Magnetically split spectra were simulated within the spin Hamiltonian formalism (22); otherwise, spectra were analyzed by least-squares fits using Lorentzian line shape.

RESULTS

Characterization of Biotin Synthase Purified from ^{57}Fe -Enriched Cells. Biotin synthase purified aerobically from *E. coli* cells overexpressing the enzyme, cultured in ^{57}Fe -enriched TB media, presented consistent values of 1.6 ± 0.1

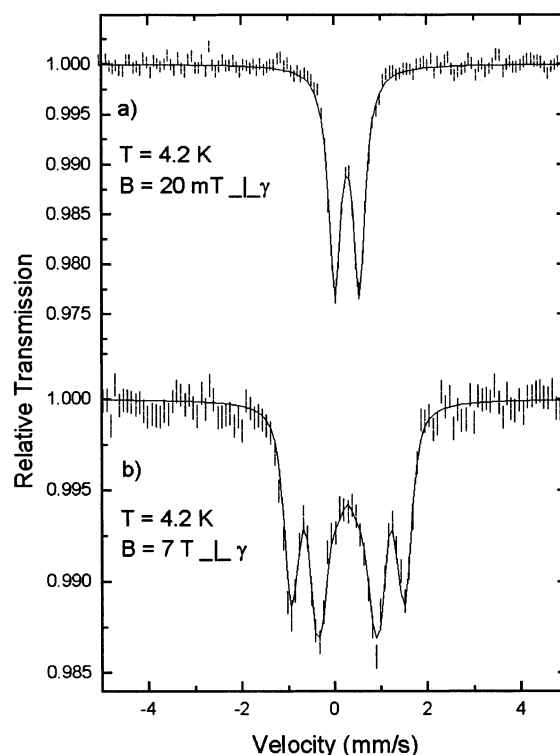


FIGURE 1: Mössbauer spectra of purified biotin synthase from overproducing strain of biotin synthase (BS+) grown in ^{57}Fe -enriched media. Spectra were recorded at 4.2 K in a field of 20 mT (a) and 7 T (b) applied perpendicular to the γ -beam. The solid line in panel a is a doublet for $[\text{2Fe-2S}]^{2+}$ with quadrupole splitting $\Delta E_Q = 0.53$ mm/s and isomer shift $\delta = 0.28$ mm/s. The solid line in panel b is a theoretical spectrum computed with values of ΔE_Q and δ obtained from panel a with the assumption that both (equivalent) Fe sites of the cluster reside in a diamagnetic environment. The simulation yielded for the asymmetry parameter the value $\eta = 1$.

Fe and $1.6 \pm 0.1 \text{ S}^{2-}$ per monomer. This amount of cluster, i.e., $0.8[\text{2Fe-2S}]^{2+}$ per monomer is what we usually obtain for the purified enzyme derived from cells grown in the same medium without addition of Fe (13).

Figure 1a shows the 4.2 K Mössbauer spectrum of the purified in vivo ^{57}Fe -labeled biotin synthase. It exhibits a doublet with quadrupole splitting $\Delta E_Q = 0.53$ mm/s and isomer shift $\delta = 0.28$ mm/s, similar to that obtained for the $[\text{2Fe-2S}]^{2+}$ cluster of the ^{57}Fe -enzyme chemically reconstituted in vitro (3). These parameters are typical for tetrahedrally sulfur-ligated high-spin Fe^{3+} with a $S = 5/2$ spin state. Application of a high field of 7 T (Figure 1b) clearly shows that the magnetic splitting is solely due to the applied field, i.e., no additional magnetic hyperfine contribution due to unpaired Fe 3d electrons is observed. This diamagnetic behavior is a consequence of the two antiparallel spin-coupled Fe^{3+} sites in a $[\text{2Fe-2S}]^{2+}$ cluster. The fit of the high-field spectrum using $\Delta E_Q = 0.53$ mm/s and $\delta = 0.28$ mm/s from the low-field measurement yields for the asymmetry parameter the value $\eta = 1$.

Characterization of Biotin Synthase in Whole Cells. The 4.2 K Mössbauer spectrum of whole cells of BS+ (Figure 2a) exhibits four doublets (Table 1). Doublet 1 represents parameters ($\Delta E_{Q,1} = 0.53$ mm/s, $\delta_1 = 0.28$ mm/s) equivalent to those found for the $[\text{2Fe-2S}]^{2+}$ clusters of biotin synthase purified from cells enriched with ^{57}Fe (Figure 1a). Doublet 2 exhibits parameters ($\Delta E_{Q,2} = 1.11$ mm/s, $\delta_2 = 0.45$ mm/s)

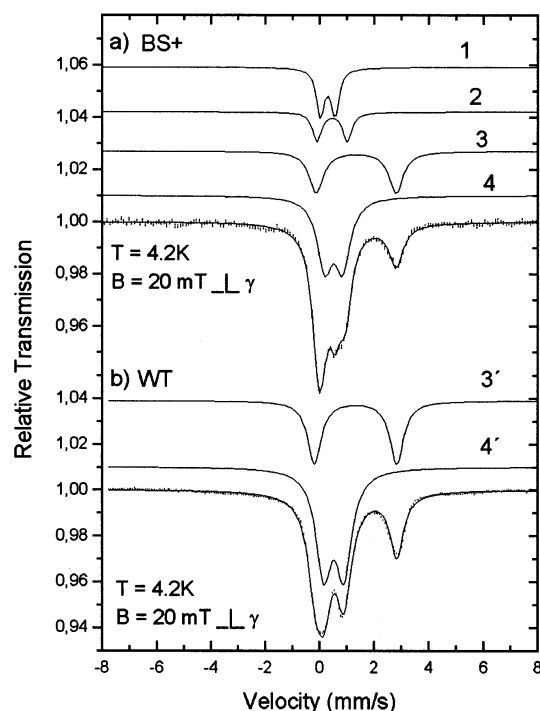


FIGURE 2: Mössbauer spectra of whole cells of *E. coli* measured at 4.2 K in a perpendicular field of 20 mT, with (a) overproducing strain of biotin synthase (BS+) and (b) the reference strain (WT). Doublet 1 represents $[2\text{Fe-2S}]^{2+}$ clusters, and doublet 2 represents $[4\text{Fe-4S}]^{2+}$ clusters. Doublets 3 and 3' belong to high-spin Fe^{2+} , and doublets 4 and 4' represent high-spin Fe^{3+} species where iron is not coordinated to sulfur. The parameters and the corresponding percentage of the absorption areas are listed in Table 1.

Table 1: Parameters for Simulations of Whole Cells Overexpressing Biotin Synthase (BS+) and of Reference Cells (WT) Shown in Figure 2

		δ (mm/s)	ΔE_Q (mm/s)	Γ (mm/s)	area (%)
BS+	1: $[2\text{Fe-2S}]^{2+}$	0.28	0.53	0.31	17
	2: $[4\text{Fe-4S}]^{2+}$	0.45	1.11	0.34	12
	3:high-spin Fe^{2+}	1.34	2.92	0.63	26
	4:high-spin Fe^{3+}	0.49	0.66	0.60	45
WT	3':high-spin Fe^{2+}	1.32	3.02	0.61	36
	4':high-spin Fe^{3+}	0.52	0.75	0.70	64

s) that are identical to $[4\text{Fe-4S}]^{2+}$ clusters of reduced biotin synthase (3). The $[2\text{Fe-2S}]^{2+}$ clusters account for 17%, and the $[4\text{Fe-4S}]^{2+}$ clusters account for 12% of the total amount of Fe. Doublet 3 has parameters ($\Delta E_{Q,3} = 2.92$ mm/s, $\delta_3 = 1.34$ mm/s) that are typical for high-spin Fe^{2+} , and doublet 4 ($\Delta E_{Q,4} = 0.66$ mm/s, $\delta_4 = 0.49$ mm/s) indicates the presence of high-spin Fe^{3+} species (in both cases, 3 and 4, the iron is not coordinated to sulfur). The last two sets of parameters have been previously reported in *E. coli* cells and suggest the presence of iron storage proteins such as ferritin (23) or compounds involved in iron metabolism (24).

Cells of the WT strain grown under the same conditions as BS+ were used as reference. Only two signals with similar parameters to 3 and 4, doublets 3' and 4' ($\Delta E_{Q,3'} = 3.02$ mm/s, $\delta_{3'} = 1.32$ mm/s and $\Delta E_{Q,4'} = 0.75$ mm/s, $\delta_{4'} = 0.52$ mm/s), were present in this case (Figure 2b).

To verify the assignments made in Figure 2, high-field measurements were performed. Figure 3, panels a and b respectively, shows the spectra of the BS+ (dashed line) and WT (squares) samples in an applied field of 7 T. The broad

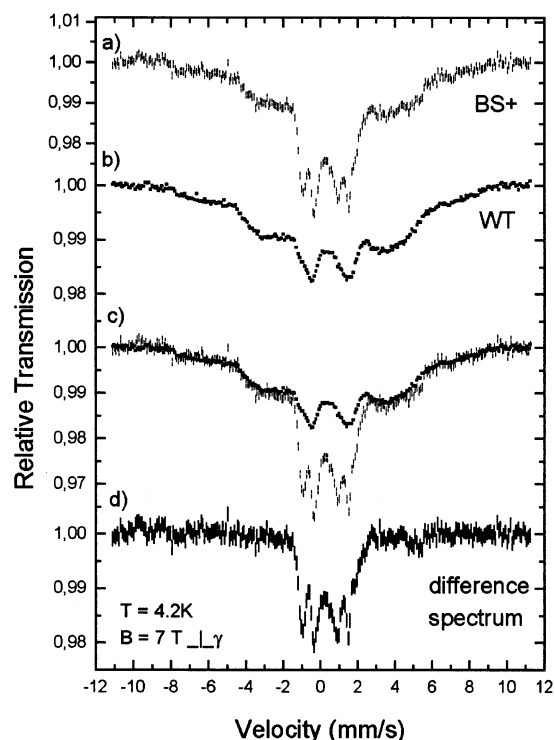


FIGURE 3: Mössbauer spectra of whole cells of *E. coli* measured at 4.2 K in a field of 7 T perpendicular to the γ -beam, with (a) overproducing strain of biotin synthase (BS+), (b) reference strain (WT), and (c) superposition of BS+ and WT. The difference spectrum (d) of BS+ and WT represents only $[\text{Fe-S}]$ clusters in BS+ cells (see text).

background in the spectra of WT and BS+ is indicative of a heterogeneous distribution of magnetically ordered species. Since in the velocity range of $11 \text{ mm/s} > |v| > 3 \text{ mm/s}$, the absorption pattern of these species is the same for both (Figure 3c), we conclude that these species show the same pattern in the whole velocity range. Therefore the difference spectrum represents $[\text{Fe-S}]$ clusters present only in the BS+ cells (Figure 3d). The observed magnetic splitting in Figure 3d is again solely due to the applied field and therefore represents diamagnetic $[2\text{Fe-2S}]^{2+}$ and $[4\text{Fe-4S}]^{2+}$ clusters.

The difference spectrum of Figure 3d displayed over a smaller velocity range is shown in Figure 4. The solid lines are simulations with parameters corresponding to diamagnetic $[2\text{Fe-2S}]^{2+}$ clusters (line 1) and diamagnetic $[4\text{Fe-4S}]^{2+}$ clusters (line 2). The fit of this difference spectrum yields relative areas of 58% for $[2\text{Fe-2S}]^{2+}$ and 42% for $[4\text{Fe-4S}]^{2+}$ clusters (Table 2). It should be noted that the relative amount of these species obtained from the high-field spectra depicted in Figure 3 is the same as that obtained from the analysis of the low-field spectra displayed in Figure 2. During this study, the low- and high-field spectra of another set of independently grown batches of cells (BS+ and WT) with similar growth conditions were recorded. The total amount of sulfur-ligated Fe found in BS in this case was 17% of the total cell iron and exhibited relative areas of 67% for $[2\text{Fe-2S}]^{2+}$ and 33% for $[4\text{Fe-4S}]^{2+}$ clusters, comparable to the cell batches shown in Figure 4. At this point, it is worth noting that our values are not far from those obtained with whole-cell Mössbauer studies of FNR (25); the total fraction of iron contained in FNR varied from 10 to 25% of total cell iron, while it varied from 17% to 29% in the present case. Thus, the analysis of the field-dependent Mössbauer spectra

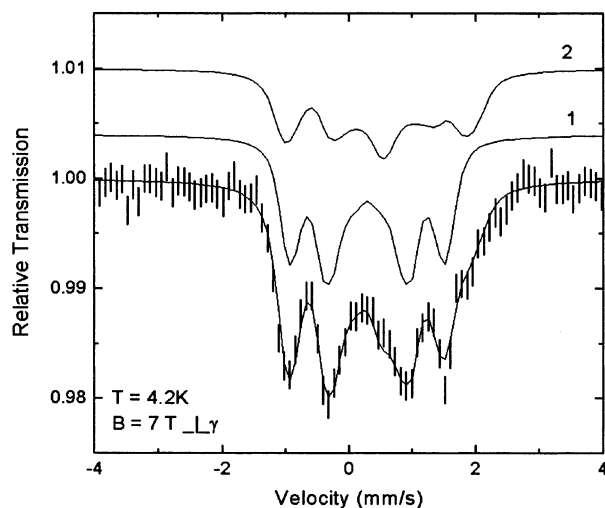


FIGURE 4: Difference spectrum of BS+ and WT measured at 4.2 K in a field of 7 T perpendicular to the γ -beam. The same spectrum is shown over a larger velocity range in Figure 3d. Line 1 represents $[2\text{Fe-2S}]^{2+}$ clusters, and line 2 represents $[4\text{Fe-4S}]^{2+}$ clusters. The solid lines are computed with values ΔE_Q and δ obtained in a field of 20 mT. For the asymmetry parameter η , the values $\eta = 1$ for $[2\text{Fe-2S}]^{2+}$ clusters and $\eta = 0.6$ for $[4\text{Fe-4S}]^{2+}$ clusters were used. The fit yields 58% for $[2\text{Fe-2S}]^{2+}$ clusters and 42% for $[4\text{Fe-4S}]^{2+}$ clusters. The obtained parameters are summarized in Table 2.

Table 2: Parameters for Simulation of Difference Spectrum of Whole Cells Overexpressing Biotin Synthase (BS+) and of Reference Cells (WT) Shown in Figure 4

	δ (mm/s)	ΔE_Q (mm/s)	Γ (mm/s)	η	area (%)
1: $[2\text{Fe-2S}]^{2+}$	0.28	0.53	0.26	1	58 (3) ^a
2: $[4\text{Fe-4S}]^{2+}$	0.45	1.11	0.35	0.6	42

^a $[2\text{Fe-2S}]^{2+}/[4\text{Fe-4S}]^{2+}$ ratio.

presented in this study shows that both $[4\text{Fe-4S}]^{2+}$ and $[2\text{Fe-2S}]^{2+}$ clusters are present in biotin synthase in vivo.

Characterization of Biotin Synthase in Crude Extracts. This mixed cluster state can still be seen in the crude extracts obtained by ultrasonication of BS+ cells, followed by centrifugation and concentration of the supernatant with a 30-kDa cutoff centrifugal concentrator, all under aerobic conditions. The 4.2 K Mössbauer spectra of crude BS+ are shown in Figure 5. The measured low-field spectrum (Figure 5a) is represented as a superposition of three quadrupole doublets: doublet 1 represents $[2\text{Fe-2S}]^{2+}$ clusters ($\Delta E_Q = 0.53$ mm/s, $\delta = 0.28$ mm/s, 40%), doublet 2 represents $[4\text{Fe-4S}]^{2+}$ clusters ($\Delta E_Q = 1.11$ mm/s, $\delta = 0.45$ mm/s, 21%), and doublet 3'' ($\Delta E_Q = 3.0$ mm/s, $\delta = 1.36$ mm/s) is characteristic for high-spin Fe^{2+} species (Table 3). These Fe^{2+} species, already observed in the whole cells, obviously were not removed by filtration while Fe^{3+} species were removed since a doublet corresponding to lines 4 and 4' was no longer observed in Figure 5a.

The measured high-field spectrum of crude BS+ (Figure 5b) is consistent with this assignment; i.e., the $[2\text{Fe-2S}]^{2+}$ and $[4\text{Fe-4S}]^{2+}$ clusters are represented by diamagnetic subspectra (line 1 and line 2), while the Fe^{2+} species is hardly visible as a broad background in the velocity range from -4 to $+4$ mm/s. From these findings we conclude that, during the preparation of the crude extracts by filtration, Fe^{3+} species were removed but not Fe^{2+} . Hence Fe^{3+} sites must

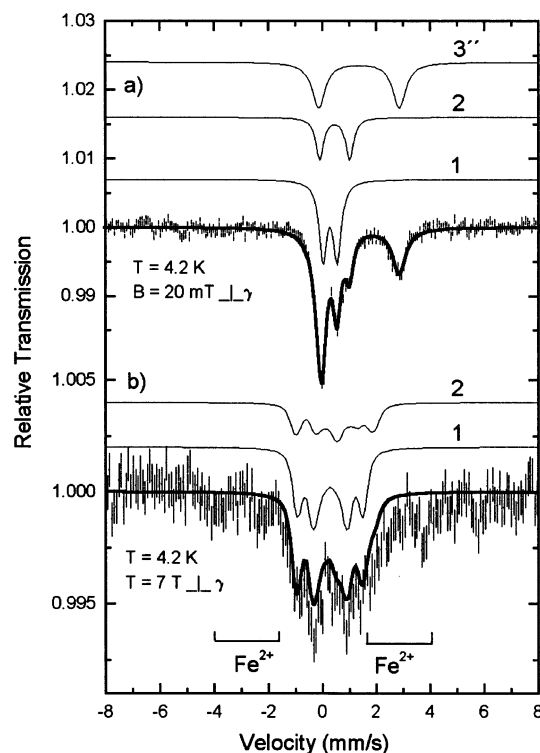


FIGURE 5: Mössbauer spectra of crude BS+ measured at 4.2 K in a perpendicular field of 20 mT (a) and 7 T (b) perpendicular to the γ -beam. Doublet 1 belongs to $[2\text{Fe-2S}]^{2+}$ clusters, doublet 2 belongs to $[4\text{Fe-4S}]^{2+}$ clusters, and doublet 3'' belongs to high-spin Fe^{2+} species. The obtained parameters are summarized in Table 3.

Table 3: Parameters for Simulations of Crude BS+ Extract Shown in Figure 5a

	δ (mm/s)	ΔE_Q (mm/s)	Γ (mm/s)	area (%)
1: $[2\text{Fe-2S}]^{2+}$	0.28	0.53	0.35	40 (4) ^a
2: $[4\text{Fe-4S}]^{2+}$	0.45	1.11	0.35	21
3'':high-spin Fe^{2+}	1.36	3.00	0.59	39

^a $[2\text{Fe-2S}]^{2+}/[4\text{Fe-4S}]^{2+}$ ratio.

belong to proteins with less than 30 kDa, according to filtration conditions, and therefore cannot correspond to ferritin (~ 500 kDa) (23) or compounds associated to iron metabolism (155 kDa) (24), as suggested above. The nonidentification of Fe^{2+} and Fe^{3+} is not at all surprising as the nature of about 75% of the iron pool in *E. coli* is still unknown (24).

It is worth noting that, although the crude extracts were prepared under aerobic conditions, the presence of the $[4\text{Fe-4S}]^{2+}$ clusters could still be observed. This is probably due to the action of oxygen-scavenging enzymes (in the crude extracts, BS comprises $\sim 10\%$ of the total soluble proteins, as determined by densitometric analysis of an electrophoresis gel stained with Coomassie Brilliant Blue R-250), which might provide a protective effect for $[4\text{Fe-4S}]^{2+}$. Contrarily, almost all $[4\text{Fe-4S}]^{2+}$ clusters were decomposed (9% $[4\text{Fe-4S}]^{2+}$ and 75% $[2\text{Fe-2S}]^{2+}$) after passage of the cell-free extracts through the first purification column using DEAE sepharose (unpublished spectrum). Since, during aerobic purification, the $[4\text{Fe-4S}]^{2+}$ clusters tend to disappear, a remedy to maintain this cluster form would be to purify the enzyme under strict anaerobic conditions.

DISCUSSION

We have used Mössbauer spectroscopy to investigate the nature of the iron–sulfur clusters of biotin synthase in vivo. Overexpression of ^{57}Fe -labeled BS was achieved by growing the *E. coli* cells aerobically with vigorous agitation till late stationary phase, in a TB medium enriched with $^{57}\text{FeCl}_3$. Mössbauer analysis of the enzyme, aerobically purified from these cells, shows that under these conditions the intracellular isotopic enrichment of BS with ^{57}Fe was high enough to obtain a well-resolved spectrum (Figure 1). The purified enzyme exhibits 100% of the $[\text{2Fe-2S}]^{2+}$ species and is devoid of adventitious iron. This method of obtaining ^{57}Fe -enriched enzyme by in vivo labeling seems to be more appropriate than the in vitro ^{57}Fe -reconstitution method, which often gives rise to additional contaminating Fe species. According to chemical analysis, the purified enzyme contains 1.6 Fe and 1.6 S^{2-} , i.e., $0.8[\text{2Fe-2S}]^{2+}$ per monomer, which is comparable to the amount of clusters we usually obtain for the pure enzyme prepared from cells grown in the same medium without addition of Fe (13).

Previous results showed that anaerobic reduction (2, 3) or reconstitution with an excess of FeCl_3 and Na_2S (14, 15) lead to $[\text{4Fe-4S}]^{2+,+}$ clusters. Air oxidation of the $[\text{4Fe-4S}]^{2+,+}$ form results in the formation of the stable $[\text{2Fe-2S}]^{2+}$ state (3, 14). It was thus interesting to investigate whether the former species existed in vivo. Therefore, Mössbauer spectroscopy was applied to whole cells of *E. coli* overexpressing BS, with the WT cells as reference. Since the background of the different iron species were identical in both samples (Figure 3), we deduced that the difference spectrum corresponded solely to $[\text{Fe-S}]$ clusters present on biotin synthase. An overexpression of other $[\text{Fe-S}]$ proteins, for instance from the *isc* operon, implicated in the biosynthesis of $[\text{Fe-S}]$ clusters (26, 27), cannot be completely excluded but should be negligible as compared to that of biotin synthase. Furthermore, these low molecular weight proteins (IscU, IscA, ferredoxin, and IscR) were eliminated during the preparation of the crude extracts.

Analysis of the aerobically grown cells shows that biotin synthase contains a mixture of $[\text{4Fe-4S}]^{2+}$ and $[\text{2Fe-2S}]^{2+}$ clusters in an approximately 1:3 ratio (Figure 4). At this point, it was interesting to investigate if the proportion of $[\text{4Fe-4S}]^{2+}$ was higher in anaerobically grown cells. Unfortunately, no overexpression of BS was observed under our experimental conditions.

This mixed cluster state is still seen in the Mössbauer spectrum of the crude cell-free extracts overexpressing biotin synthase (Figure 5). Although these extracts were obtained under aerobic conditions, the presence of $[\text{4Fe-4S}]^{2+}$ was still detectable in a $[\text{4Fe-4S}]^{2+}:[\text{2Fe-2S}]^{2+}$ ratio of 1:4. As expected, aerobic purification of BS gives rise to a decrease in the amount of $[\text{4Fe-4S}]^{2+}$; a first anion-exchange column yielded an enzyme fraction with a $[\text{4Fe-4S}]^{2+}:[\text{2Fe-2S}]^{2+}$ ratio of 1:17 and further purification led to the pure enzyme, which is completely devoid of $[\text{4Fe-4S}]^{2+}$.

Jarrett and co-workers (16, 28) recently obtained by in vitro reconstitution an enzyme containing a mixture of $[\text{2Fe-2S}]^{2+}$ and $[\text{4Fe-4S}]^{2+}$ clusters in a 1:0.8 ratio. Their Mössbauer study using differentially substituted ^{57}Fe protein indicated that the two clusters bind at distinct sites. These authors also reported that this mixed cluster state was

essential for optimal activity in vitro. Using UV–visible spectroscopy and quantitative iron and sulfide analysis, they observed that the $[\text{2Fe-2S}]^{2+}$ cluster was destroyed whereas the $[\text{4Fe-4S}]^{2+}$ cluster was preserved during enzymatic reaction. Our previous results showing the incorporation of ^{34}S into biotin from an $[\text{Fe-}^{34}\text{S}]$ -reconstituted enzyme indicated that the $[\text{Fe-S}]$ center was the sulfur source for biotin (13). Of course, these experiments did not address the question of the nature of the sulfur-donating cluster. The results of Jarrett and co-workers suggest that the $[\text{4Fe-4S}]^{2+}$ cluster could be involved in radical generation by mediating the reductive cleavage of AdoMet into DOA $^{\bullet}$ while the $[\text{2Fe-2S}]^{2+}$ could be the immediate source of sulfur in biotin.

Interestingly, we also observed the presence of the two types of clusters in biotin synthase in vivo. Purification of the enzyme under strict anaerobic conditions, which is under way in our laboratory, will enable us to further characterize the protein, in particular, to verify if it has the same properties as the reconstituted enzyme. Although not strictly demonstrated, it is tempting to assume that the mixed cluster state is also the active form in vivo.

To date, in vivo Mössbauer spectroscopy has been widely applied to obtain information on the intracellular iron pool and on iron uptake and metabolism in a number of microorganisms (29–31). Some time ago, Münck and co-workers (25) demonstrated for the first time that ^{57}Fe Mössbauer spectroscopy could be used to study the structure of $[\text{Fe-S}]$ clusters of FNR expressed to $\sim 5\%$ in whole cells of *E. coli*. With this study, we present a second example of a successful application of this technique to the in vivo characterization of $[\text{Fe-S}]$ clusters.

ACKNOWLEDGMENT

We thank Pr. Y. Izumi for the generous gift of *E. coli* strains.

REFERENCES

1. Sanyal, I., Cohen, G., and Flint, D. H. (1994) *Biochemistry* 33, 3625–3631.
2. Duin, E. C., Lafferty, M. E., Crouse, B. R., Allen, R. M., Sanyal, I., Flint, D. H., and Johnson, M. K. (1997) *Biochemistry* 36, 11811–11820.
3. Tse Sum Bui, B., Florentin, D., Marquet, A., Benda, R., and Trautwein, A. X. (1999) *FEBS Lett.* 459, 411–414.
4. McIver, L., Baxter, R. L., and Campopiano, D. J. (2000) *J. Biol. Chem.* 275, 13888–13894.
5. Hewitson, K. S., Baldwin, J. E., Shaw, N. M., and Roach, P. L. (2000) *FEBS Lett.* 466, 372–376.
6. Ugulava, N. B., Gibney, B. R., and Jarrett, J. T. (2001) *Biochemistry* 40, 8343–8351.
7. Ifuku, O., Kishimoto, J., Haze, S., Yanagi, M., and Fukushima, S. (1992) *Biosci. Biotechnol. Biochem.* 56, 1780–1785.
8. Florentin, D., Tse Sum Bui, B., Marquet, A., Ohshiro, T., and Izumi, Y. (1994) *C. R. Acad. Sci. Paris, Life Sci.* 317, 485–488.
9. Ifuku, O., Koga, N., Haze, S., Kishimoto, J., and Wachi, Y. (1994) *Eur. J. Biochem.* 224, 173–178.
10. Birch, O. M., Fuhrmann, M., and Shaw, N. M. (1995) *J. Biol. Chem.* 270, 19158–19165.
11. Guianvarc'h, D., Florentin, D., Tse Sum Bui, B., Nunzi, F., and Marquet, A. (1997) *Biochem. Biophys. Res. Commun.* 236, 402–406.
12. Escalantes, F., Florentin, D., Tse Sum Bui, B., Lesage, D., and Marquet, A. (1999) *J. Am. Chem. Soc.* 121, 3571–3578.
13. Tse Sum Bui, B., Florentin, D., Fournier, F., Ploux, O., Méjean, A., and Marquet, A. (1998) *FEBS Lett.* 440, 226–230.
14. Ollagnier-de Choudens, S., Sanakis, Y., Hewitson, K. S., Roach, P., Baldwin, J. E., Münck, E., and Fontecave, M. (2000) *Biochemistry* 39, 4165–4173.
15. Ugulava, N. B., Gibney, B. R., and Jarrett, J. T. (2000) *Biochemistry* 39, 5206–5214.

16. Ugulava, N. B., Sacanell, C. J., and Jarrett, J. T. (2001) *Biochemistry* 40, 8352–8358.
17. Ohshiro, T., Yamamoto, M., Tse Sum Bui, B., Florentin, D., Marquet, A., and Izumi, Y. (1995) *Biosci. Biotechnol. Biochem.* 59, 943–944.
18. Neidhardt, F. C., Bloch, P. L., and Smith, D. F. (1974) *J. Bacteriol.* 119, 736–747.
19. Bradford, M. M. (1976) *Anal. Biochem.* 72, 248–254.
20. Fish, W. W. (1998) *Methods Enzymol.* 158, 357–364.
21. Beinert, H. (1983) *Anal. Biochem.* 131, 373–378.
22. Trautwein, A. X., Bill, E., Bominaar, E. L., and Winkler, H. (1991) *Struct. Bonding* 78, 1–95.
23. Hudson, A. J., Andrews, S. C., Hawkins, C., Williams, J. M., Izuhara, M., Meldrum, F. C., Mann, S., Harrison, P. M., and Guest, J. R. (1993) *Eur. J. Biochem.* 218, 985–995.
24. Matzanke, B. F., Müller, G. I., Bill, E., and Trautwein, A. X. (1989) *Eur. J. Biochem.* 183, 371–379.
25. Popescu, C., Bates, D. M., Beinert, H., Münck, E., and Kiley, P. J. (1998) *Proc. Natl. Acad. Sci. U.S.A.* 95, 13431–13435.
26. Frazzon, J., and Dean, D. R. (2001) *Proc. Natl. Acad. Sci. U.S.A.* 26, 14751–14752.
27. Tokumoto, U., and Takahashi, Y. (2001) *J. Biochem.* 130, 63–71.
28. Ugulava, N. B., Surerus, K. K., and Jarrett, J. T. (2002) *J. Am. Chem. Soc.* 124, 9050–9051.
29. Matzanke, B. F., Bill, E., and Trautwein, A. X. (1991) *Hyperfine Interact.* 71, 1259–1262.
30. Matzanke, B. F., Berner, I., Bill, E., Trautwein, A. X., and Winkelmann, G. (1991) *Biol. Metals* 4, 181–185.
31. Matzanke, B. F., Böhnke, R., Möllmann, U., Reissbrodt, R., Schünemann, V., and Trautwein, A. X. (1998) *BioMetals* 11, 1–11.

BI026590Q